

**This item is the archived peer-reviewed author-version of:**

Comparison of a universal (but complex) model for avian egg shape with a simpler model

**Reference:**

Shi Peijian, Gielis Johan, Niklas Karl J..- Comparison of a universal (but complex) model for avian egg shape with a simpler model  
Annals of the New York Academy of Sciences / New York Academy of Sciences - ISSN 1749-6632 - 1514:1(2022), p. 34-42  
Full text (Publisher's DOI): <https://doi.org/10.1111/NYAS.14799>  
To cite this reference: <https://hdl.handle.net/10067/1884700151162165141>

**ANNALS** *of* THE NEW YORK  
ACADEMY OF SCIENCES

**Comparison of a recently published universal model for  
avian egg shape with a simpler model**

Journal:	<i>Ann NY Acad Sci</i>
Manuscript ID	annals--115
Manuscript Type:	Commentary
Date Submitted by the Author:	24-Feb-2022
Complete List of Authors:	Shi, Peijian; Nanjing Forestry University, Bamboo Research Institute, College of Science, GIELIS, Johan; University of Antwerp, Biosciences Engineering Niklas, Karl J.; Cornell University, School of Integrative Plant Science
Keywords:	goodness-of-fit, model structure, Narushin- Romanov-Griffin equation, simplified Gielis equation, symmetry

SCHOLARONE™  
Manuscripts

1  
2  
3  
4 1 **Comparison of a recently published universal model for avian egg shape with a**  
5  
6 2 **simpler model**

7  
8 3  
9  
10 4 Peijian Shi,<sup>1</sup> Johan Gielis,<sup>2</sup> and Karl J. Niklas<sup>3</sup>

11  
12 5  
13  
14 6 <sup>1</sup>Bamboo Research Institute, Nanjing Forestry University, Nanjing 210037, China.

15  
16 7 <sup>2</sup>Department of Biosciences Engineering, University of Antwerp, Groenenborgerlaan,

17  
18 8 B-2020 Antwerpen, Belgium. <sup>3</sup>School of Integrative Plant Science, Cornell University,

19  
20 9 Ithaca, NY 14853, USA.

21  
22 10  
23  
24 11 Correspondence: Johan Gielis, E-mail: johan.gielis@uantwerpen.be

25  
26 12 Department of Biosciences Engineering, University of Antwerp, Groenenborgerlaan,

27  
28 13 B-2020 Antwerpen, Belgium.

29  
30 14  
31  
32 15 **Short title:** Comparison of two egg shape models

33  
34 16  
35  
36 17 **Keywords:** goodness-of-fit; model structure; Narushin- Romanov-Griffin equation,

37  
38 18 simplified Gielis equation; symmetry; universality

39  
40 19  
41  
42  
43  
44  
45  
46  
47  
48  
49  
50  
51  
52  
53  
54  
55  
56  
57  
58  
59  
60

1  
2  
3  
4 20 **Abstract**

5  
6 21 Recently a universal model, called NRGE, was proposed to describe the shape of avian  
7  
8 22 eggs. It can simulate the shape of spherical, ellipsoidal, ovoidal, and pyriform eggs.  
9  
10 23 However, the predictions of NRGE were not tested against actual data. Here, we tested  
11  
12 24 the validity of NRGE by fitting actual data of egg shapes, and compared it with the  
13  
14 25 predictions of a simpler model for egg shape (denoted as SGE). The eggs of nine bird  
15  
16 26 species were sampled for this purpose. NRGE was found to fit the empirical data of egg  
17  
18 27 shape well, but it did not define the egg length axis (i.e., symmetric axis) which  
19  
20 28 significantly affected the prediction accuracy. The egg length axis in NRGE is defined  
21  
22 29 as the maximum distance between two points on the scanned perimeter of the egg's  
23  
24 30 shape. In contrast, SGE fitted the empirical data better, and had a smaller root-mean-  
25  
26 31 square error than NRGE for each of the nine eggs. Based on its mathematical simplicity  
27  
28 32 and goodness of fit, SGE appears to be a reliable and useful model for egg shape.  
29

30 33  
31  
32  
33  
34  
35  
36  
37  
38  
39  
40  
41  
42  
43  
44  
45  
46  
47  
48  
49  
50  
51  
52  
53  
54  
55  
56  
57  
58  
59  
60

## 35 Introduction

36

37 Bird eggs manifest excellent axial symmetry, i.e., their shapes are perfectly symmetric  
 38 along a well-defined length axis. Yet, avian eggs are asymmetric along their maximum  
 39 width axis, which has attracted the attention of many scientists interested in modelling  
 40 natural shape.<sup>1-3</sup> For example, Stoddard et al.<sup>1</sup> proposed two biologically relevant  
 41 parameters, asymmetry and ellipticity, to quantify diverse egg shapes. The concept of  
 42 asymmetry is a relative measure for the extent of the deviation from a circle or an ellipse  
 43 in one direction since all eggs share bilateral symmetry in their top-down cross-section.  
 44 In a recent publication,<sup>2</sup> a universal equation (denoted henceforth as **NRGE**) for  
 45 simulating different shapes of eggs was proposed by Narushin, Romanov and Griffin  
 46 who substantially extended Hügelschäffer's formula to render their new equation to  
 47 describe the shape of pyriform eggs:

48

$$\begin{aligned}
 y = & \pm \frac{B}{2} \sqrt{\frac{(L^2 - 4x^2)}{(L^2 + 8Lw - 4w^2)}} \times \\
 & \left[ 1 - \frac{\sqrt{5.5L^2 + 11Lw + 4w^2} \times (\sqrt{3BL} - 2D_{L/4} \sqrt{L^2 + 2Lw + 4w^2})}{\sqrt{3BL}(\sqrt{5.5L^2 + 11Lw + 4w^2} - 2\sqrt{L^2 + 2Lw + 4w^2})} \times \right. \\
 & \left. \left( 1 - \sqrt{\frac{L(L^2 + 8wx + 4w^2)}{2(L-2w)x^2 + (L^2 + 8Lw - 4w^2)x + 2Lw^2 + L^2w + L^3}} \right) \right] \quad (1)
 \end{aligned}$$

49

50 where  $x$  and  $y$  represent the abscissa and ordinate of the egg shape in the Euclidean  
 51 coordinate system,  $L$  represents the egg's length,  $B$  represents the egg's maximum  
 52 width,  $w$  is  $(L-W) / 2k$ , where  $k$  is a positive number to be estimated, and  $D_{L/4}$  is the  
 53 egg's diameter at the distance of  $L/4$  from the tip of the egg.

54

55 Narushin *et al.*<sup>2</sup> simulated different egg shapes by adjusting the numerical value  
 56 of parameter  $w$ , and compared the simulations with seven actual egg shapes. In this

57 important and seminal work, NERGE is transformed to deal with the basic ovoid forms  
 58 (i.e., spherical, ellipsoidal, and Hügelschäffer's ovoid), which can be deemed as a  
 59 'mathematical evolution' from the simplest shape (i.e., sphere) to the most complex  
 60 (i.e., Hügelschäffer's ovoid). However, they did not provide the results of fitting the  
 61 empirical data of egg shape. They only demonstrated the feasibility of NERGE in  
 62 depicting the diversity of egg shape by simulation. Thus, there is a need to test whether  
 63 NERGE can effectively approximate actual egg shapes and to evaluate the goodness-of-  
 64 fit. In addition, although Eq. (1) is described as being 'universal' in simulating the shape  
 65 of avian eggs, its applied scope is limited to a certain class of shapes.

66 It is also necessary to consider alternative equations for the purpose of simulating  
 67 egg shape, as for example the equation proposed by Johan Gielis,<sup>4</sup> which describes  
 68 many organic shapes especially symmetric ones:

$$r(\varphi) = a \left( \left| \cos\left(\frac{m}{4}\varphi\right) \right|^{n_2} + k \left| \sin\left(\frac{m}{4}\varphi\right) \right|^{n_3} \right)^{-1/n_1}, \quad (2)$$

70 where  $r$  is the polar radius at the polar angle  $\varphi$ , where  $a$ ,  $k$ ,  $n_1$ ,  $n_2$  and  $n_3$  are parameters  
 71 to be estimated, and  $m$  is a positive integer, which determines the number of angles of  
 72 the curve generated by Eq. (2) within  $[0, 2\pi]$ . This is a generalization of the Pythagorean  
 73 Theorem and of the superellipse equation.<sup>4</sup> When  $n_2 = n_3$ , Eq. (2) produces bilaterally  
 74 symmetric shapes, and when  $n_2 = n_3$ ,  $k = 1$  and  $m > 1$ , Eq. (2) produces radial symmetric  
 75 shapes. Many classical geometries such as circles, ellipses, squares, rectangles,  
 76 diamonds, triangles, and pentagrams can be generated by Eq. (2). The simplified Gielis  
 77 equation has been used to successfully fit the empirical outline data of bamboo leaves,  
 78 sea stars, seeds, and tree rings.<sup>5-9</sup>

80 Prior work on a variety of organic shapes (e.g., the seeds of *Ginkgo biloba*, the  
 81 Maidenhair tree)<sup>9</sup> indicates that Eq. (2) can be simplified further when dealing with  
 82 objects manifesting near perfect bilateral symmetry (e.g.,  $m = 1$ ), i.e.,

83

$$r(\varphi) = a \left( |\cos(\varphi/4)|^{n_2} + |\sin(\varphi/4)|^{n_2} \right)^{-1/n_1}, \quad (3)$$

84

85 which has only three parameters,  $a$ ,  $n_1$ , and  $n_2$ . Note that the abscissa and ordinate of  
86 egg shape in the Euclidean coordinate system can be calculated as  $x = r \cos \varphi$  and  $y =$   
87  $r \sin \varphi$ , respectively. Eq. (3) is denoted as SGE (simplified Gielis equation) hereafter.

88

89 Here, we compare the ability of NRGE and SGE to fit the empirical data of the  
90 egg shapes of nine species of birds spanning the full range of egg shapes to determine  
91 which of these two models is more successful at fitting the empirical data.

92

### 93 **Data Acquisition and Parameter Estimation**

94

95 We used the shapes of seven eggs appearing in Ref. 2, and added two additional egg  
96 shapes (see Fig. 1 for details). The protocols proposed by Su *et al.*<sup>10</sup> were subsequently  
97 used to extract the planar coordinates of these shapes to obtain 2000–3000 data points  
98 for each the perimeter of the egg's shape.

99

100 Because the planar coordinates of the scanned images usually deviated from those  
101 generated by SGE (Fig. 2), three additional location parameters were introduced, i.e.,  
102  $x_0$ ,  $y_0$ , and  $\theta$ ,<sup>5-9</sup> where  $(x_0, y_0)$  represents the coordinates of the polar point of SGE in the  
103 Euclidean coordinate system, and  $\theta$  represents the angle between the scanned egg length  
104 axis (i.e., the major axis) and the  $x$ -axis. The value of  $\theta$  was defined as a positive number  
105 when the major axis rotated counterclockwise from the  $x$ -axis, and it was defined as a  
106 negative number when the major axis rotated clockwise from the  $x$ -axis. To estimate  
107 the parameters of SGE, we minimized the residual sum of squares between the actual  
108 distances from the polar point to the data points on the scanned the perimeter of the  
109 egg's shape and the distances from the polar point to the data points on the predicted  
110 perimeter of the egg's shape using the Nelder-Mead optimization method.<sup>11</sup>

111

112 Due to the complexity of the mathematical structure of NRGE, the Nelder-Mead  
113 optimization method failed to estimate the parameters. Because three out of four  
114 parameters of NRGE have clear biological and geometric meanings (i.e.,  $L$ ,  $B$  and  $D_{L/4}$ ),  
115 their values could be estimated by means of numerical calculation. After obtaining the  
116 numerical values of the three parameters, the optimization method was used to estimate  
117  $w$ . Because of the failure of using the optimization method to estimate the major axis  
118 and model parameters of NRGE, it was difficult to define the egg length axis, although  
119 it is essential for calculating  $L$ ,  $B$  and  $D_{L/4}$ . For this reason, two methods were used to  
120 obtain the major axis: the maximum distance method, and the SGE major axis  
121 approximation method. In the first method, the straight line through two points forming  
122 the maximum distance on the perimeter of the egg's shape is defined as the major axis.  
123 In the second method, the major axis predicted by SGE was directly used as the major  
124 axis of NRGE, because SGE balances the goodness-of-fit of the model and the bilateral  
125 symmetry of the curve. Because the direction from the egg base to the egg tip predicted  
126 by SGE is the reverse of that predicted by NRGE, the angle between the major axis of  
127 NRGE and the  $x$ -axis is equal to the sum of the estimated  $\theta$  of SGE and  $\pi$ .

128

129 Once the major axis is established, the distance of the major axis can be calculated  
130 as the estimate of  $L$ . Using the maximum distance method,  $L$  equals the maximum  
131 distance. Using the SGE major axis approximation method,  $L$  may be slightly smaller  
132 than the true distance. After rotating the major axis to make it overlap with the  $x$ -axis,  
133 a large number of equidistant rectangles can be used<sup>12</sup> (e.g., 2000) from the egg base to  
134 egg tip to intersect the perimeter of the egg's shape. This methodology makes it easy to  
135 obtain the maximum egg width (i.e.,  $B$ ) and  $D_{L/4}$ . The residual sum of squares (RSS)  
136 between the observed and predicted  $y$  values can be minimized using the optimization  
137 method to estimate  $w$ . Despite the complex structure of NRGE [see Eq. (1)], the  
138 optimization method for estimating the remaining parameter  $w$  becomes feasible after  
139 the other three parameters were numerically estimated.

140



1  
2  
3  
4 141 The root-mean-square error (RMSE) between the observed and predicted ordinate  
5  
6 142 coordinates,  $y_i$  and  $\hat{y}_i$ , respectively, was used to determine the goodness-of-fit of any  
7  
8 143 of the two models:  
9

10 144

$$\text{RMSE} = \sqrt{\sum_{i=1}^N (y_i - \hat{y}_i)^2 / N}, \quad (4)$$

14 145

16 146 where the subscript  $i$  represent the  $i$ th data point on the egg's edge, and  $N$  represents  
17  
18 147 the number of data points on the egg's edge. As a rule of thumb, a  $\leq 0.05$  RMSE  
19  
20 148 indicates a satisfying goodness-of-fit of a model, thereby validating a model's ability  
21  
22 149 to fit the data. We compared NRGE with SGE based on their RMSE values. If SGE has  
23  
24 150 a smaller RMSE, it can be concluded that SGE is superior in its goodness-of-fit and its  
25  
26 151 model simplicity.

27  
28  
29 152 The software R (version 4.1.2)<sup>13</sup> was used to carry out all calculations and data  
30  
31 153 fitting.

32  
33 154

## 35 155 **Results and Discussion**

36  
37 156

38  
39 157 Analyses indicated that the RMSE values obtained using SGE are smaller than 0.05 for  
40  
41 158 each of the nine egg shapes investigated (Fig. 3 and Table S1 in online supplementary  
42  
43 159 material). There are two methods to define the major axis of NRGE (i.e., the maximum  
44  
45 160 distance method and the SGE major axis approximation method) that can be used to  
46  
47 161 numerically calculate the model's parameters. The RMSE of NRGE based on the first  
48  
49 162 method was higher than the RMSE of NRGE based on the second method (Figs. 4 and  
50  
51 163 5; Tables S2 and S3). Therefore, the SGE major axis approximate method is better to  
52  
53 164 find the major axis of the egg shape generated by NRGE, which can improve the  
54  
55 165 goodness-of-fit. However, the two methods are only for the use of NRGE. The RMSE  
56  
57 166 values of the two methods for NRGE were both higher than the RMSE values obtained  
58  
59 167 using SGE for each of the nine egg shapes (Tables S2 and S3 vs. Table S1). The

1  
2  
3  
4 168 maximum distance method obtained a large prediction error for the egg of *Uria aalge*  
5  
6 169 (i.e.,  $RMSE = 0.1821$ ), whereas  $RMSE = 0.0335$  using the SGE major axis  
7  
8 170 approximation method. These results support the validity of NRGE in light of empirical  
9  
10 171 data for egg shape once the major axis was properly identified. However, as can be  
11  
12 172 seen, the selection of the major axis relies on the predictions of SGE. It should be noted  
13  
14 173 that we were unable to directly find the optimal major axis of NRGE based on the  
15  
16 174 optimization method due to the complexity of model's structure. To directly use the  
17  
18 175 straight line associated with the maximum distance between two points on an egg-edge  
19  
20 176 was infeasible for several egg shapes. In addition, we found that the estimates of  
21  
22 177 parameter  $w$  in NRGE obtained negative numbers for several eggs (see Tables S2 and  
23  
24 178 S3), which was inconsistent with how  $w$  was originally defined in NRGE (i.e.,  $k$  is  
25  
26 179 considered to be a positive number to be estimated).<sup>2</sup>  
27  
28  
29

30 181 The NRGE has revealed a mathematical 'evolution' from the simplest shape (i.e.,  
31  
32 182 sphere) to the most complex (i.e., Hügelschäffer's ovoid), and the predicted curves  
33  
34 183 exhibited a good axi-symmetry and covered the ovoid geometries of interest. Given the  
35  
36 184 morphological similarity between reptilian eggs and bird eggs, NRGE also applies to  
37  
38 185 both types, and it is likely applicable for describing the shape of some insect eggs.  
39  
40 186 However, although SGE has fewer parameters, its goodness-of-fit is better than that of  
41  
42 187 NRGE. In general, the fewer the number of parameters, the more concise a model and  
43  
44 188 the greater the 'close-to-linear' behavior in the relevant nonlinear regression, i.e., the  
45  
46 189 greater the convergence in the parameter space using fewer data points.<sup>14-16</sup> In our  
47  
48 190 study, Akaike information criteria or Bayesian information criteria (which consider the  
49  
50 191 trade-off between the goodness-of-fit and the complexity of model's structure<sup>17</sup>) were  
51  
52 192 not used to compare SGE with NRGE, because the mathematical simplicity of SGE  
53  
54 193 with fewer parameters clearly obtains smaller RMSE values than NRGE. Overall, from  
55  
56 194 the viewpoint of the conciseness of model structure and goodness-of-fit, SGE offers  
57  
58 195 advantages over NRGE. It is also necessary to point out that the purported universality  
59  
60

1  
2  
3  
4 196 of NRGE is constrained regarding its range of egg geometries. By relaxing the  
5  
6 197 limitation for  $m = 1$  in Eq. (3), the four-parameter SGE with the same number of  
7  
8 198 parameters as NRGE can describe a broader range of geometries including triangles,  
9  
10 199 rectangles, pentagrams, and others, i.e., the ‘universality’ of SGE is greater than that of  
11  
12 200 NRGE.

13  
14 201 It is useful to point out that it is not feasible to use a one-parameter model to  
15  
16 202 adequately describe the shape of eggs. Indeed, a two-parameter SGE was required to  
17  
18 203 describe the shape of bamboo leaves, i.e.,<sup>5,6,18</sup>

19  
20 204

$$r(\varphi) = a \left( |\cos(\varphi/4)| + |\sin(\varphi/4)| \right)^{-1/n_1}, \quad (5)$$

21  
22 205

23  
24  
25  
26 206 where the parameters  $a$  and  $n_1$  were empirically found to represent leaf length and width,  
27  
28 207 which implies that Eq. (5) can be considered as a function of leaf length and width.<sup>10,</sup>

29  
30 208 <sup>18</sup> Although Eq. (5) was shown to be valid for fitting the empirical data of bamboo  
31  
32 209 leaves,<sup>5,6,18</sup> it cannot be extended to other ovate or lanceolate leaf shapes.<sup>18</sup> We explored

33  
34 210 the use of Eq. (5) to fit the actual data of the egg shapes shown in Fig. 1, but failed to  
35  
36 211 confirm its universality across all of the nine egg shapes (results not shown because of

37  
38 212 the space limitations). However, a two-parameter SGE can reflect a limited spectrum  
39  
40 213 of egg shapes by setting  $n_2$  to be a constant (as done in Eq. [5]) whose numerical value

41  
42 214 relies on the morphological characteristics of the class of egg shapes of interest.  
43  
44 215 However, it is clear that such a two-parameter SGE cannot serve as a universal formula

45  
46 216 for egg shape. In fact, the length and width of a planar projection of a biological object  
47  
48 217 with a certain intra-variation in morphology can estimate the area of the projection, by

49  
50 218 multiplying the product of length and width with a parameter to be estimated.<sup>19, 20</sup> This  
51  
52 219 suggests to us that the parameter can be potentially regarded as an index to quantify

53  
54 220 shape by checking the extent of deviation from a rectangle or an ellipse.<sup>21</sup> However,  
55  
56 221 this parameter does not reflect the extent of symmetry for the shape of interest.<sup>1</sup>

57  
58 222 Therefore, any viable ‘universal’ model for egg shape must consider the extent of the  
59  
60

223 deviation from a given geometry (e.g., an ellipse) and that of symmetry or asymmetry.  
224 In that case, a truly universal model for egg shape requires three or more parameters.

225

## 226 **Conclusion**

227

228 The validity of the Narushin-Romanov-Griffin equation (NRGE) with four parameters  
229 was confirmed for fitting the empirical data of nine species of bird eggs representing  
230 the full spectrum of avian egg shapes. However, the prediction accuracy of NRGE  
231 depends on whether the major axis (i.e., the egg length axis) can be correctly  
232 determined. Because of the complexity of the NRGE model, the parameters of NRGE  
233 cannot be directly estimated using optimization methods. A simplified Gielis equation  
234 with three parameters (SGE) was proposed to describe the shape of avian eggs, and its  
235 validity was confirmed. Specifically, the goodness-of-fit of SGE is greater than that of  
236 NRGE for each of the nine egg shapes. Given the conciseness of SGE model and its  
237 lower root-mean-square errors relative to NRGE, SGE is advocated as a better  
238 ‘universal’ model for egg shape. In addition, if we add an additional parameter  $m$  in  
239 SGE, it can generate a broader spectrum of geometries than NRGE. After using the  
240 predicted major axis by SGE, the prediction error of NRGE was greatly decreased  
241 relative to that using the straight line identified by the maximum distance between two  
242 points on the perimeter of the egg’s shape as the major axis. The future application of  
243 NRGE would benefit by using SGE to predict the major axis. Although NRGE and SGE  
244 both provide feasible tools for describing and fitting the actual shape of avian (and non-  
245 avian) eggs, SGE is more concise and more flexible in its curve-fitting capacity.

246

## 247 **Author contributions**

248 P.S. and J.G. were both involved in conceptualization, formal analysis, investigation,  
249 methodology, and writing. J.G. was also involved in supervision. K.J.N. was involved  
250 in formal analysis, investigation, and editing.

251

**252 Acknowledgements**

253 We thank Valerity G. Narushin for his valuable discussion on the main results of this  
254 work, and Yirong Li for her helpful image processing work. We also thank Dr. Douglas  
255 Braaten for encouraging us to submit this work for publication.

256

**257 Supporting information**

258 Additional supporting information may be found in the online version of this  
259 manuscript.

260 **Table S1.** Fitted results using the simplified Gielis equation (SGE) to the nine eggs

261 **Table S2.** Fitted results using the Narushi-Romanov-Griffin equation (NRGE) based  
262 on the maximum distance method to the nine eggs

263 **Table S3.** Fitted results using the Narushi-Romanov-Griffin equation (NRGE) based  
264 on the SGE major axis approximation method to the nine eggs

265

**266 Competing interests**

267 The authors declare no competing interests.

268

**269 References**

- 270 1. Stoddard, M.C., E.H. Yong, D. Akkaynak, *et al.* 2017. Avian egg shape: Form,  
271 function, and evolution. *Science* **356**: 1249–1254.
- 272 2. Narushin, V.G., M.N. Romanov & D.K. Griffin. 2021. Egg and math: introducing  
273 a universal formula for egg shape. *Ann. N.Y. Acad. Sci.* 1505: 169–177.
- 274 3. Biggins, J.D., J.E. Thompson & T.R. Birkhead. 2018. Accurately quantifying the  
275 shape of birds' eggs. *Ecol. Evol.* **8**: 9728–9738.
- 276 4. Gielis, J., 2003. A generic geometric transformation that unifies a large range of  
277 natural and abstract shapes. *Am. J. Bot.* **90**: 333–338.
- 278 5. Shi, P., Q. Xu, H.S. Sandhu, *et al.* 2015. Comparison of dwarf bamboos  
279 (*Indocalamus* sp.) leaf parameters to determine the relationship between the spatial  
280 density of plants and total leaf area per plant. *Ecol. Evol.* **5**: 4578–4589.

- 281 6. Lin, S., Zhang, L., Reddy, G.V.P., *et al.* 2016. A geometrical model for testing  
282 bilateral symmetry of bamboo leaf with a simplified Gielis equation. *Ecol. Evol.* **6**:  
283 6798–6806.
- 284 7. Shi, P., Ratkowsky, D.A. & Gielis, J. 2020. The generalized Gielis geometric  
285 equation and its application. *Symmetry***12**: 645.
- 286 8. Shi, P., J. Huang, C. Hui, *et al.* 2015. Capturing spiral growth of conifers using  
287 superellipse to model tree-ring geometric shape. *Front. Plant Sci.* **6**: 856.
- 288 9. Tian, F., Wang, Y., Sandhu, H.S., *et al.* 2020. Comparison of seed morphology of  
289 two ginkgo cultivars. *J. For. Res.* **31**: 751–758.
- 290 10. Su, J., Niklas, K.J., Huang, W., *et al.* 2019. Lamina shape does not correlate with  
291 lamina surface area: An analysis based on the simplified Gielis equation. *Glob.*  
292 *Ecol. Conser.* **19**: e006666.
- 293 11. Nelder, J.A. & R. Mead. 1965. A simplex algorithm for function minimization.  
294 *Comput. J.* **7**: 308–313.
- 295 12. Shi, P., X. Zheng, D.A. Ratkowsky, *et al.* 2018. A simple method for measuring the  
296 bilateral symmetry of leaves. *Symmetry* **10**: 118.
- 297 13. R Core Team. 2021. *R: A Language and Environment for Statistical Computing*.  
298 Vienna, Austria: R Foundation for Statistical Computing. Accessed February 1  
299 2021. <https://www.R-project.org/>.
- 300 14. Bates, D.M & Watts, D.G. 1988. *Nonlinear Regression Analysis and its*  
301 *Applications*. New York, NY: Wiley.
- 302 15. Ratkowsky, D.A. 1990. *Handbook of Nonlinear Regression Models*. New York,  
303 NY: Marcel Dekker.
- 304 16. Ratkowsky, D.A. & Reddy, G.V.P. 2017. Empirical model with excellent statistical  
305 properties for describing temperature-dependent developmental rates of insects and  
306 mites. *Ann. Entomol. Soc. Am.* **110**: 302–309.
- 307 17. Spiess, A.-N. & Neumeier, N. 2010. An evaluation of R squared as an inadequate  
308 measure for nonlinear models in pharmacological and biochemical research: a  
309 Monte Carlo approach. *BMC Pharmacol.* **10**: 6.
- 310 18. Shi, P., Ratkowsky, D.A., Li, Y., *et al.* 2018. General leaf-area geometric formula  
311 exists for plants – Evidence from the simplified Gielis equation. *Forests* **9**: 714.
- 312 19. Shi, P., Liu, M., Ratkowsky, D.A., *et al.* 2019. Leaf area-length allometry and its  
313 implications in leaf-shape evolution. *Trees Struct. Funct.* **33**: 1073–1085.

1  
2  
3 314 20. Yu, X., Shi, P., Schrader, J., *et al.* 2020. Nondestructive estimation of leaf area for  
4  
5 315 15 species of vines with different leaf shapes. *Am. J. Bot.* **107**: 1481–1490.

6  
7 316 21. Li, Y., Quinn, B.K., Niinemets, Ü., *et al.* 2021. Ellipticalness index — A simple  
8  
9 317 measure for the complexity of oval leaf shape. *Pak. J. Bot.* in press.

10  
11 318  
12  
13  
14  
15  
16  
17  
18  
19  
20  
21  
22  
23  
24  
25  
26  
27  
28  
29  
30  
31  
32  
33  
34  
35  
36  
37  
38  
39  
40  
41  
42  
43  
44  
45  
46  
47  
48  
49  
50  
51  
52  
53  
54  
55  
56  
57  
58  
59  
60

Unedited manuscript

1  
2  
3  
4 319 **Figure legends**

5  
6 320 **Figure 1.** Nine eggs used to assess modeling capability. The egg of *Gallus gullus* was  
7  
8 321 photographed by Peijian Shi; a common murre egg came from the website  
9  
10 322 ([https://www.penbaypilot.com/article/kristen-lindquist-everyday-miracle-bird-](https://www.penbaypilot.com/article/kristen-lindquist-everyday-miracle-bird-egg/117278)  
11  
12 323 [egg/117278](https://www.penbaypilot.com/article/kristen-lindquist-everyday-miracle-bird-egg/117278)); the others came from the websites reported in Ref. 2. The actual size of  
13  
14 324 each was calculated using the scale in the corresponding original image.

15  
16 325 **Figure 2.** Comparison between the coordinates of a scanned egg shape with those of  
17  
18 326 the egg shape generated by the simplified Gielis equation. The polar coordinates of the  
19  
20 327 scanned egg shape are  $(-1, 1)$  and  $\theta = -\pi/4$ . The major axis (red straight line) of the  
21  
22 328 scanned egg shape can be considered as a result of a straight line on the  $x$ -axis rotating  
23  
24 329 clockwise  $\pi/4$ .

25  
26 330 **Figure 3.** Comparison between the scanned egg shape and that predicted by the  
27  
28 331 simplified Gielis equation (SGE) with three parameters to the nine egg examples.  
29  
30 332 RMSE represents the root-mean-square error; the gray curve is the scanned egg shape  
31  
32 333 (i.e., actual egg's shape); the red curve is the predicted egg shape by the model.

33  
34 334 **Figure 4.** Comparison between the scanned egg shape and that predicted by the  
35  
36 335 Narushi-Romanov-Griffin equation (NRGE) with four parameters, based on the  
37  
38 336 maximum distance method, to the nine egg examples. RMSE represents the root-mean-  
39  
40 337 square error; the gray curve is the scanned egg shape (i.e., actual egg shape); the red  
41  
42 338 curve is the predicted egg shape by the model.

43  
44 339 **Figure 5.** Comparison between the scanned egg shape and that predicted by the  
45  
46 340 Narushi-Romanov-Griffin equation (NRGE) with four parameters, based on the SGE  
47  
48 341 major axis approximation method, to the nine egg examples. RMSE represents the root-  
49  
50 342 mean-square error; the gray curve is the scanned egg shape (i.e., actual egg shape); the  
51  
52 343 red curve is the predicted egg shape by the model.

53  
54 344





*Turdus philomelos*



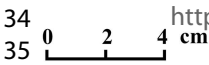
*Gallus gallus*



*Uria aalge*



*Gallinago media*



*Pandion haliaetus*

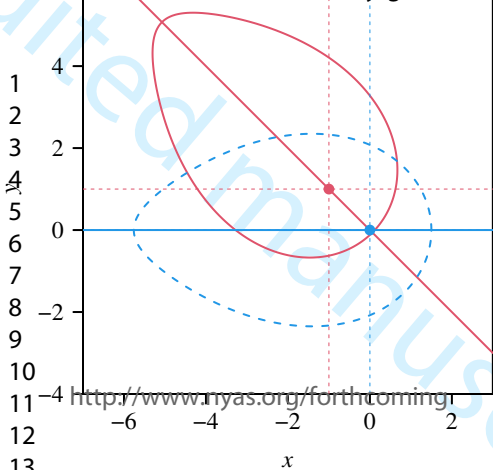


*Uria lomvia*

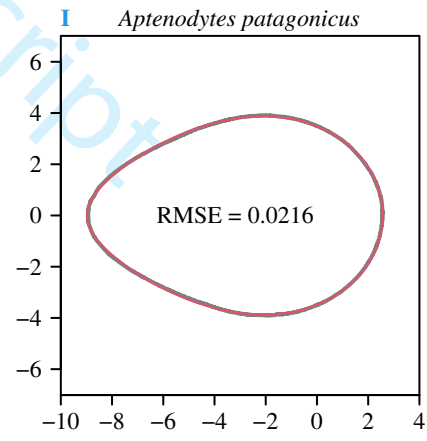
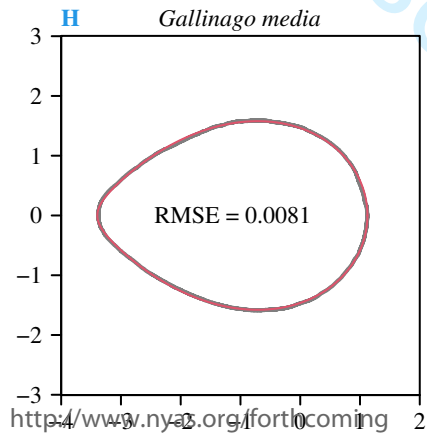
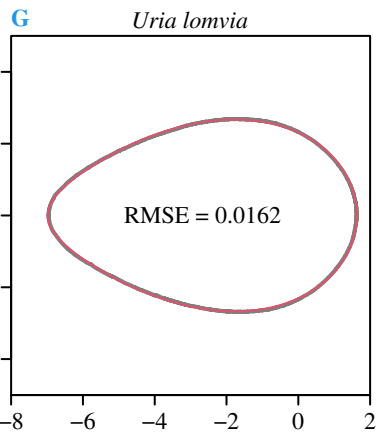
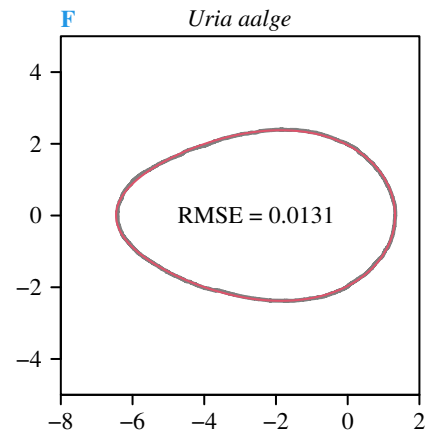
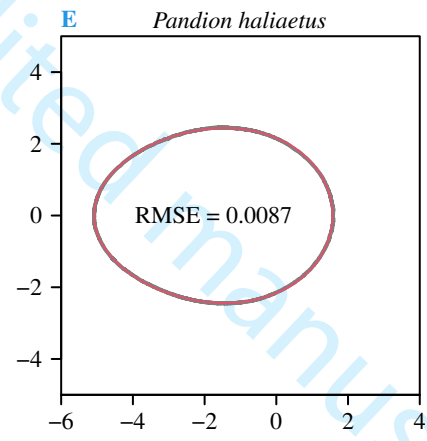
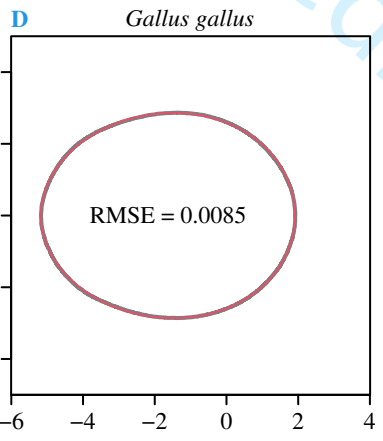
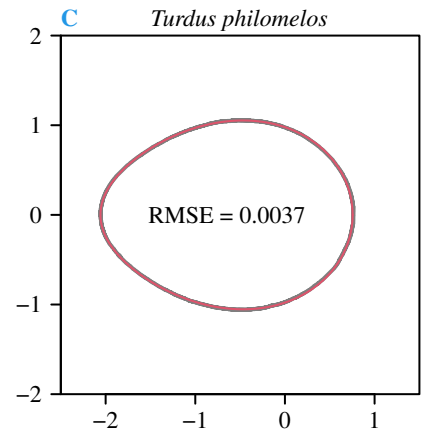
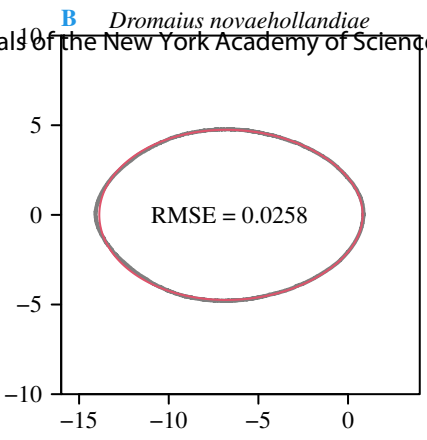
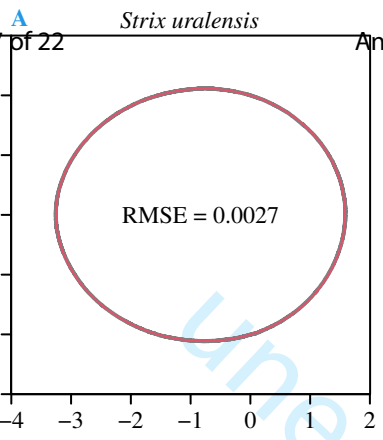


*Aptenodytes patagonicus*

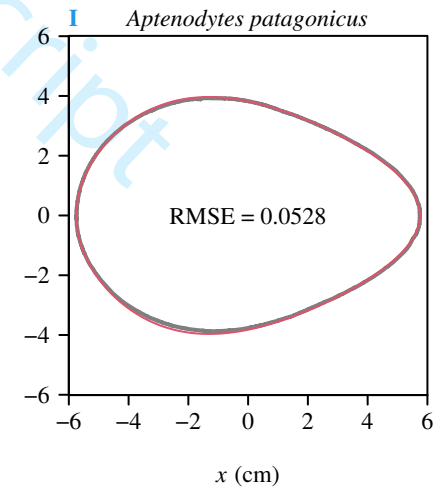
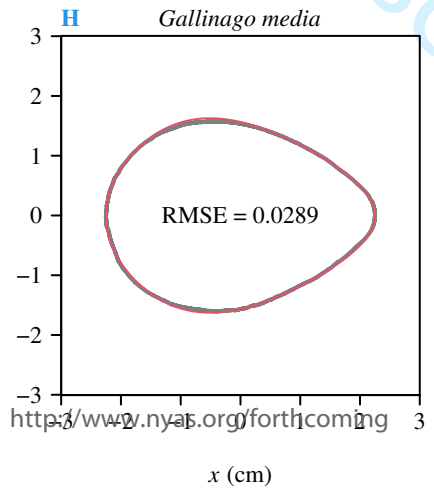
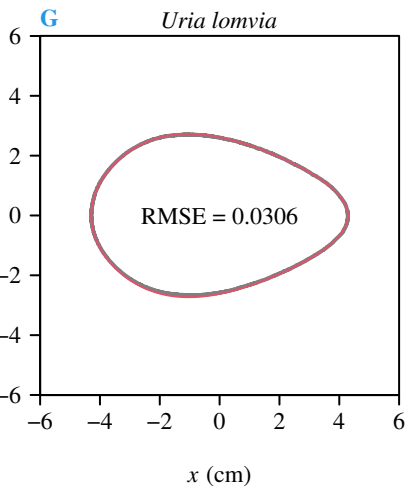
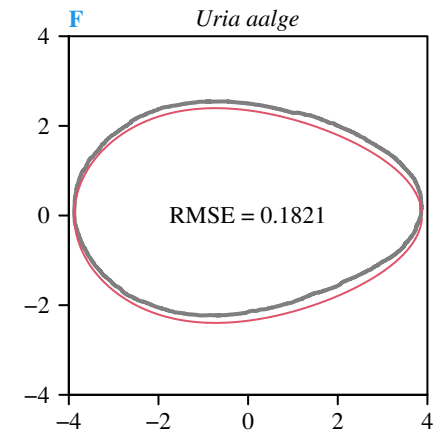
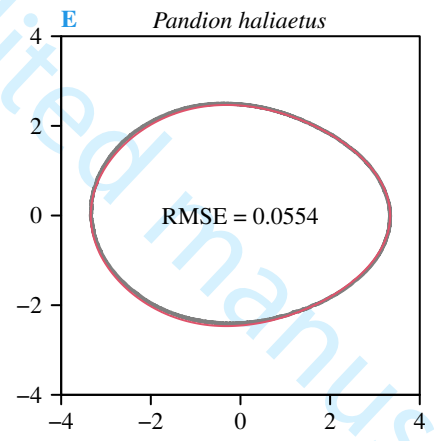
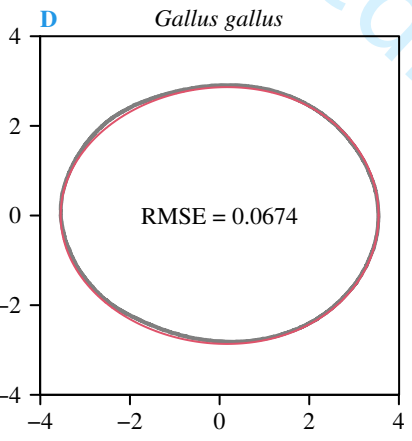
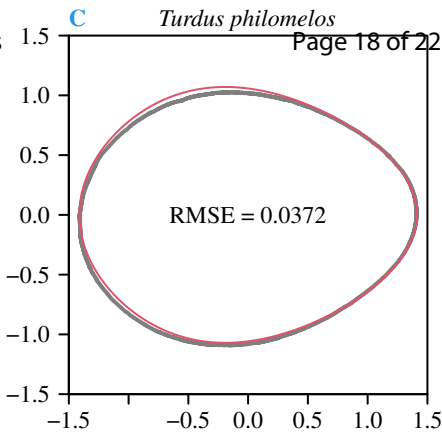
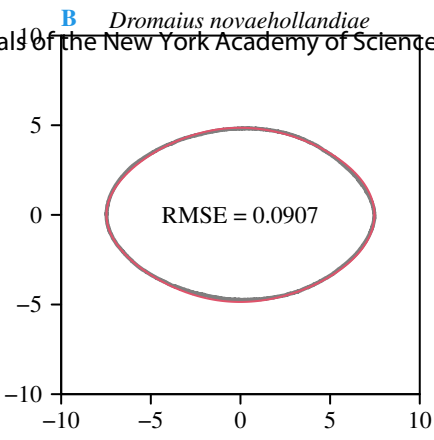
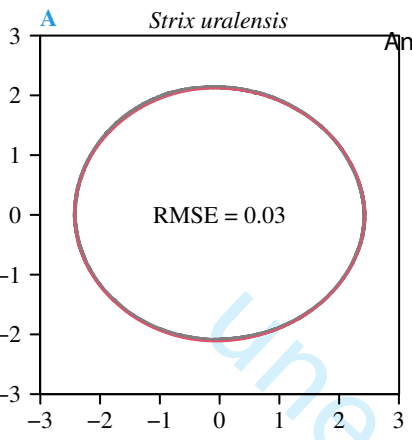




1  
2  
5  
6  
7  
8  
9  
10  
11  
12  
13  
14  
15  
16  
17  
18  
19  
20  
21  
22  
23  
24  
25  
26  
27  
28  
29  
30  
31  
32  
33  
34  
35  
36  
37  
38  
39  
40  
41

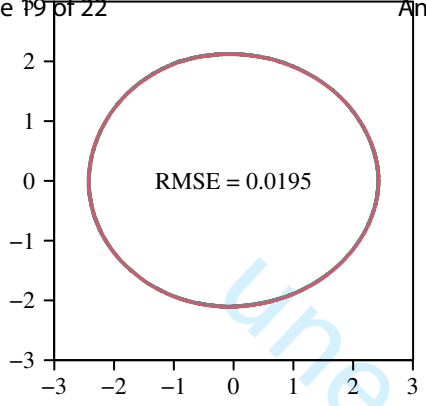


1  
2  
5  
6  
7  
8  
9  
10  
11  
12  
13  
14  
15  
16  
17  
18  
19  
20  
21  
22  
23  
24  
25  
26  
27  
28  
29  
30  
31  
32  
33  
34  
35  
36  
37  
38  
39  
40  
41

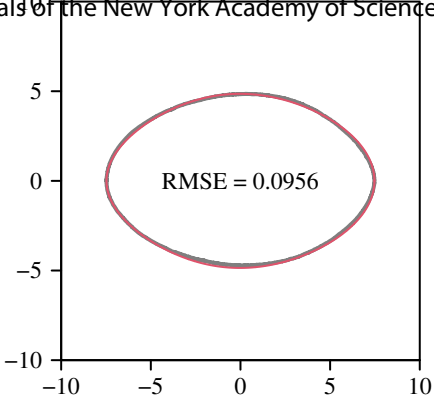


1  
2  
5  
6  
7  
8  
9  
10  
11  
12  
13  
14  
15  
16  
17  
18  
19  
20  
21  
22  
23  
24  
25  
26  
27  
28  
29  
30  
31  
32  
33  
34  
35  
36  
37  
38  
39  
40  
41

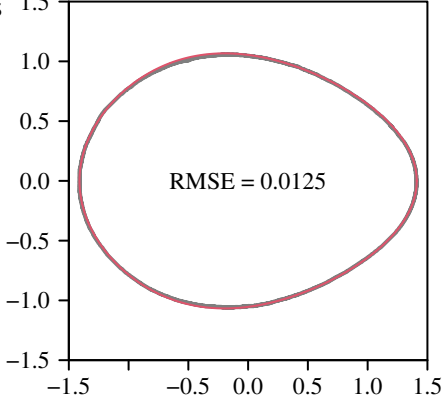
**A** *Strix uralensis*



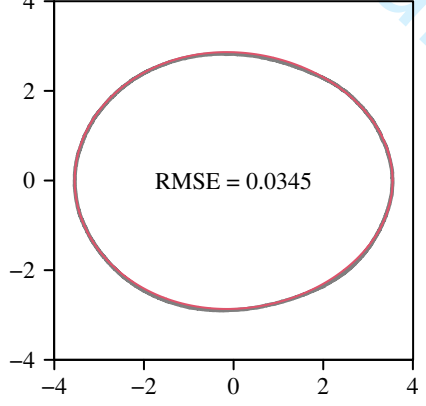
**B** *Dromaius novaehollandiae*



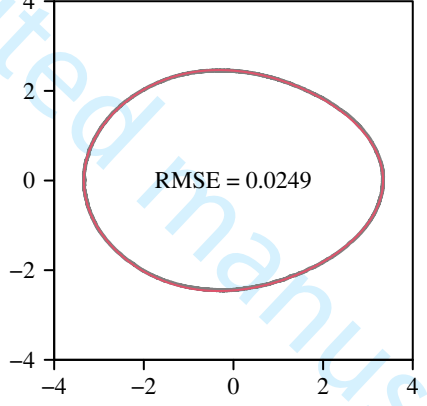
**C** *Turdus philomelos*



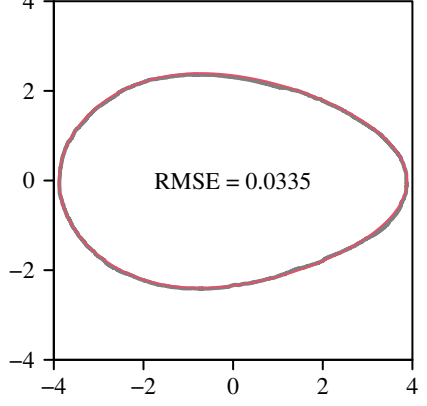
**D** *Gallus gallus*



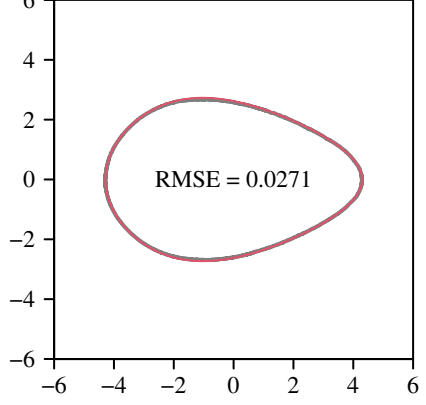
**E** *Pandion haliaetus*



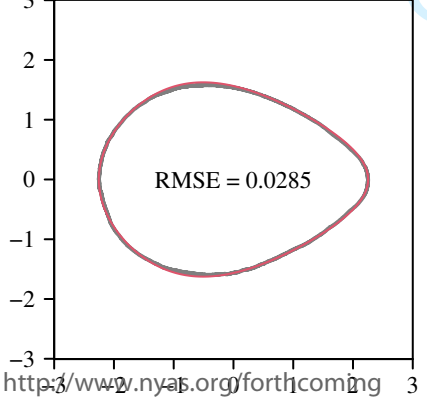
**F** *Uria aalge*



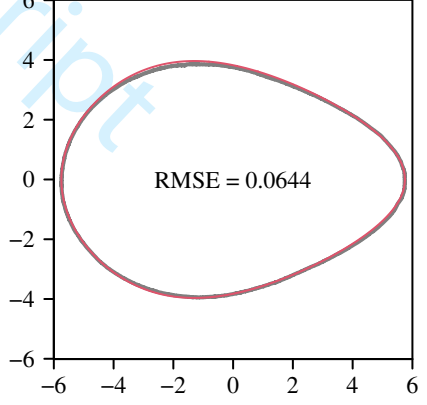
**G** *Uria lomvia*



**H** *Gallinago media*



**I** *Aptenodytes patagonicus*



x (cm)

x (cm)

x (cm)

**Table S1.** Fitted results using the simplified Gielis equation (SGE) to the nine eggs

<b>Species</b>	<b><math>x_0</math></b>	<b><math>y_0</math></b>	<b><math>\theta</math></b>	<b><math>a</math></b>	<b><math>n_1</math></b>	<b><math>n_2</math></b>	<b>Length</b>	<b>Width</b>	<b>Area</b>	<b>RSS</b>	<b><math>N</math></b>
<i>Strix uralensis</i>	19.0838	19.0105	3.8352	1.5836	2.2409	6.6471	4.8505	4.2351	16.0189	0.0217	2996
<i>Dromaius novaehollandiae</i>	44.9468	42.5071	3.9444	0.8104	0.5398	6.4232	14.9470	9.5761	108.9956	1.9919	2999
<i>Turdus philomelos</i>	9.7020	9.6087	3.9332	0.7548	5.2122	17.0839	2.8212	2.1175	4.5517	0.0290	2075
<i>Gallus gallus</i>	29.5917	25.7853	6.2615	1.9101	2.0557	7.9118	7.0920	5.7293	31.8526	0.2183	2999
<i>Pandion haliaetus</i>	22.0227	21.4504	3.9467	1.5644	2.8869	11.8125	6.6750	4.9101	25.2994	0.2261	2990
<i>Uria aalge</i>	30.6614	23.9197	0.0096	1.3204	4.5965	23.0556	7.7560	4.7776	28.3091	0.5147	2997
<i>Uria lomvia</i>	26.4530	25.4271	3.9511	1.6239	8.6162	38.2804	8.5816	5.3748	34.3207	0.7850	2999
<i>Gallinago media</i>	14.7791	14.7885	3.9306	1.1246	14.8388	49.3067	4.5062	3.1801	10.5849	0.1976	2999
<i>Aptenodytes patagonicus</i>	35.1851	35.6391	3.9365	2.5630	8.5660	33.0040	11.4956	7.8058	66.9549	1.4039	2997

1  
2  
3  
4  
5  
6  
7  
8  
9  
10  
11  
12  
13  
14  
15  
16  
17  
18  
19  
20  
21  
22  
23  
24  
25  
26  
27  
28  
29  
30  
31  
32  
33  
34  
35  
36  
37  
38  
39  
40  
41  
42  
43  
44  
45  
46

**Table S2.** Fitted results using the Narushi-Romanov-Griffin equation (NRGE) based on the maximum distance method to the nine eggs

Species	$\theta$	$L$	$B$	$w$	$D_{L/4}$	Length	Width	Area	RSS	$N$
<i>Strix uralensis</i>	0.7286	4.8523	4.2315	-0.0227	3.6050	4.8523	4.2315	16.0189	2.6885	2996
<i>Dromaius novaehollandiae</i>	0.8088	14.9473	9.5693	-1.1107	8.1660	14.9473	9.5693	108.9956	24.6551	2999
<i>Turdus philomelos</i>	0.7387	2.8235	2.1191	0.0160	1.6509	2.8235	2.1191	4.5517	2.8735	2075
<i>Gallus gallus</i>	0.0215	7.0924	5.7284	-0.1211	5.0786	7.0924	5.7284	31.8526	13.6214	2999
<i>Pandion haliaetus</i>	0.8433	6.6789	4.9097	0.0136	3.9787	6.6789	4.9097	25.2994	9.1708	2990
<i>Uria aalge</i>	3.1301	7.7560	4.7714	0.4136	3.6339	7.7560	4.7714	28.3091	99.3389	2997
<i>Uria lomvia</i>	0.8151	8.5818	5.3736	0.4044	3.7727	8.5818	5.3736	34.3207	2.8120	2999
<i>Gallinago media</i>	0.7781	4.5062	3.1799	0.1242	2.2262	4.5062	3.1799	10.5849	2.5102	2999
<i>Aptenodytes patagonicus</i>	0.8023	11.4959	7.8037	0.4571	5.5542	11.4959	7.8037	66.9549	8.3699	2997

\* Note: Here  $\theta$  was estimated to be the angle between the straight line associated with the maximum distance between two points on the egg edge and the  $x$ -axis.

**Table S3.** Fitted results using the Narushi-Romanov-Griffin equation (NRGE) based on the SGE major axis approximation method to the nine eggs

Species	$\theta$	$L$	$B$	$w$	$D_{L/4}$	Length	Width	Area	RSS	$N$
<i>Strix uralensis</i>	6.9767	4.8505	4.2337	-0.0095	3.5993	4.8505	4.2337	16.0189	1.1362	2996
<i>Dromaius novaehollandiae</i>	7.0860	14.9470	9.5685	-1.0963	8.1588	14.9470	9.5685	108.9956	27.3804	2999
<i>Turdus philomelos</i>	7.0748	2.8212	2.1166	0.0369	1.6498	2.8212	2.1166	4.5517	0.3257	2075
<i>Gallus gallus</i>	9.4031	7.0920	5.7291	0.0802	4.8449	7.0920	5.7291	31.8526	3.5727	2999
<i>Pandion haliaetus</i>	7.0883	6.6750	4.9082	0.0365	3.9757	6.6750	4.9082	25.2994	1.8499	2990
<i>Uria aalge</i>	3.1512	7.7560	4.7713	0.4008	3.6390	7.7560	4.7713	28.3091	3.3581	2997
<i>Uria lomvia</i>	7.0927	8.5816	5.3729	0.4057	3.7722	8.5816	5.3729	34.3207	2.2072	2999
<i>Gallinago media</i>	7.0721	4.5062	3.1798	0.1242	2.2291	4.5062	3.1798	10.5849	2.4286	2999
<i>Aptenodytes patagonicus</i>	7.0781	11.4956	7.8030	0.4449	5.5605	11.4956	7.8030	66.9549	12.4250	2997

\* Note: Here  $\theta$  is equal to the estimated  $\theta$  of SGE +  $\pi$ .